

Gaussian Mixture Reduction with Composite Transportation Divergence

Qiong Zhang, Archer Gong Zhang, Jiahua Chen

Abstract

Gaussian mixtures can approximate almost any smooth density function and are used to simplify downstream inference tasks. As such, it is widely used in applications in density estimation, belief propagation, and Bayesian filtering. In these applications, a finite Gaussian mixture provides an initial approximation to density functions that are updated recursively. A challenge in these recursions is that the order of the Gaussian mixture increases exponentially, and the inference quickly becomes intractable. To overcome the difficulty, the Gaussian mixture reduction, which approximates a high order Gaussian mixture by one with a lower order, can be used. Existing methods such as the clustering-based approaches are renowned for their satisfactory performance and computationally efficiency. However, they have unknown convergence and optimal targets. We propose a novel optimization-based Gaussian mixture reduction method. We develop a majorization-minimization algorithm for its numerical computation and establish its theoretical convergence under general conditions. We show many existing clustering-based methods are special cases of ours, thus bridging the gap between optimization-based and clustering-based methods. The unified framework allows users to choose the most suitable cost function to achieve superior performance in their specific application. We demonstrate the efficiency and effectiveness of the proposed method through extensive empirical experiments.

Index Terms

Approximate inference, Belief propagation, Density approximation, Gaussian mixture reduction, Optimal transportation.

I. INTRODUCTION

FINITE mixture model is a probabilistic model for the presence of finitely many subpopulations in the entire population but the observed data have no direct information about which subpopulations they came from. They are ideal tools for model-based clustering [1–3] in areas such as image processing and information processing in communication networks [4]. A finite mixture distribution is a convex combination of finitely many distinct distributions from a parametric distribution family. Among them, the finite Gaussian mixture model (GMM) is the most widely used mixture in applications due to many nice properties of the Gaussian distribution. Let $\phi(x; \mu, \Sigma) = |2\pi\Sigma|^{-1/2} \exp\{-(x - \mu)^\top \Sigma^{-1}(x - \mu)/2\}$ be the density function of a d -dimensional Gaussian distribution. We exchangeably write $\phi(x; \mu, \Sigma) = \phi(x; \theta)$ with $\theta = (\mu, \Sigma) \in \Theta = \mathbb{R} \times S_d^+$ where S_d^+ denotes the space of $d \times d$ symmetric positive definite matrices. Let $G = \sum_{n=1}^N w_n \delta_{\theta_n}$ be a probability measure that assigns probability $w_n > 0$ to $\theta_n = (\mu_n, \Sigma_n)$ for $n \in [N] = \{1, 2, \dots, N\}$ where $\theta_n \neq \theta_{n'}$ for $n \neq n'$. We denote the density function of a finite Gaussian mixture of order N by

$$\phi(x; G) = \sum_{n=1}^N w_n \phi(x; \theta_n) = \int \phi(x; \theta) dG(\theta). \quad (1)$$

We call G mixing distribution, w_n mixing weight, and θ_n subpopulation or component parameter. We prefer parameterizing GMM with a mixing distribution G rather than a vector such as $(w_1, \dots, w_K, \theta_1, \dots, \theta_K)^\top$ because the mixing distribution G does not suffer from the well-known label-switching dilemma [5, Section 1.14]. We will highlight the advantage of employing G further in Section III-A.

Mixture models are also widely used because they can precisely approximate almost any smooth density functions [6], which is known as the universal approximation property [7]. This property leads to many applications in approximate inference such as belief propagation [8, 9] and Bayesian filtering [10]. In these applications, a finite Gaussian mixture is used to provide an initial approximation to density functions that are updated recursively. A challenge in these recursions is that the order of the Gaussian mixture increases exponentially and the inference quickly becomes computationally intractable. To overcome the difficulty, the technique called Gaussian mixture reduction (GMR), which approximates a high-order Gaussian mixture by one with lower-order, can be used. As seen in Fig. 1, the density function of an 8-component mixture in (a) is well approximated by a 3-component mixture in (b). One could hence use GMR to replace a high-order GMM with a lower-order GMM after each update, thereby reducing the computational cost in downstream operations. More specifically, GMR approximates a given mixture $\phi(x; G) = \sum_{n=1}^N w_n \phi(x; \theta_n)$ by a lower order mixture ($M \ll N$)

$$\phi(x; \tilde{G}) = \sum_{m=1}^M \tilde{w}_m \phi(x; \tilde{\theta}_m).$$

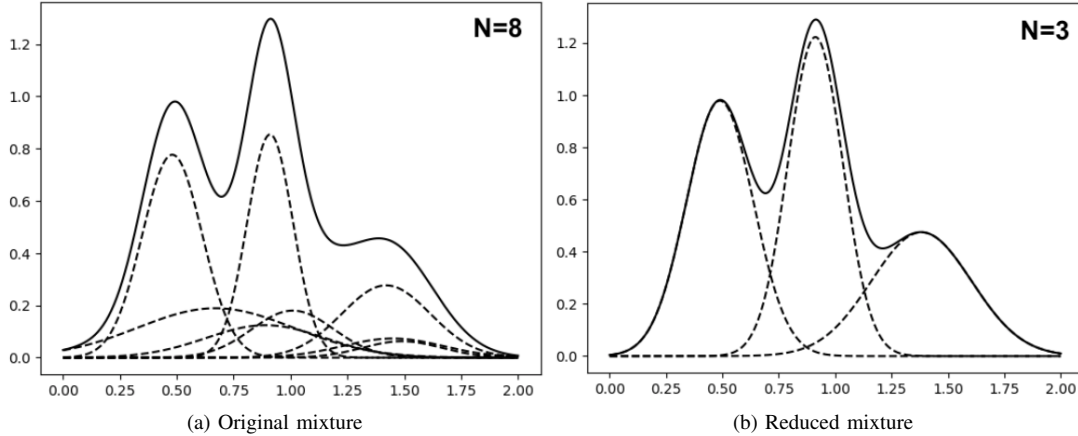


Fig. 1: Two Gaussian mixtures of different orders have similar shaped density functions (solid line). The dashed lines are subpopulation density functions.

We refer to two mixtures $\phi(x; G)$ and $\phi(x; \tilde{G})$ as the original mixture and the reduced mixture respectively. We assume the target order M is pre-specified.

There exist at least three general types of GMR approaches in the literature: *greedy algorithm-based* [11, 12], *optimization-based* [13, 14], and *clustering-based* approaches [10, 15–20]. The greedy algorithms are easy to implement. They usually use *ad-hoc* similarity metrics [21] and the outcomes are destined to be sub-optimal. In comparison, the optimization-based approaches have a well-defined optimality target. However, the optimization itself can be computationally expensive and notoriously slow when the GMM has a large dimension d or reduction order M or both. The clustering-based approaches are computationally efficient and inspired by the popular k -means algorithm [22]. Despite the computational efficiency, their optimality target and convergence properties remain unknown to the best of our knowledge.

This paper bridges the gap between the optimization-based and clustering-based approaches for GMR. We highlight the following contributions.

- First, we propose a novel optimization-based approach for GMR. We target at minimizing a composite transportation divergence [23, 24] between the original and the reduced mixtures. The composite transportation divergence leverages the computational efficiency on the divergence between two Gaussian subpopulations. In comparison, many divergences between two Gaussian mixtures employed in existing approaches are harder to evaluate and minimize over.
- Second, we develop a novel, computationally efficient majorization-minimization (MM) algorithm to solve the optimization problem. We prove that the MM algorithm converges under general conditions.
- Third, we show that many existing clustering-based approaches are special cases of our MM algorithm. As a byproduct, we establish the theoretical convergence of these existing clustering-based algorithms and reveal that their hidden optimality targets are the composite transportation divergence to the original mixture. This discovery bridges the gap between optimization-based and clustering-based algorithms for GMR.

In conclusion, our GMR approach has a well-motivated optimality target and permits effective numerical solutions. The remainder of the paper is organized as follows. In Section II, we overview the existing approaches for GMR. In Section III, we formally define the composite transportation divergence, the proposed GMR method, and the corresponding MM algorithm. We point out that many existing clustering-based methods are special cases of our MM algorithm. The unified framework permits the users to choose the most suitable cost functions to achieve superior performance in their specific applications. We compare different approaches by numerical experiments in Section IV. Section V concludes the paper.

II. EXISTING METHODS FOR MIXTURE REDUCTION

We are aware of three general categories of existing methods: greedy algorithm, optimization, and clustering-based approaches. We briefly review these methods in this section and refer interested readers to [21] for a more thorough review.

A. Greedy algorithm-based

[11, 12, 25] contain representative greedy algorithm-based methods. The top-down greedy algorithm-based methods typically either merge two components, or prune one component of the original mixture at a time until the desired order is obtained. The bottom-up greedy algorithm-based methods usually start from a single Gaussian and add one subpopulation at-a-time until reaching the desired order. If merging two components, one approach usually selects the most similar pair of components and merges them via moment matching. The pruning method either discards the component with the smallest weight, or

discards the component with the lowest “cost” to remove, and then adjusts the weights of the remaining components. Greedy methods usually require an *ad-hoc* similarity measure [21]. They strive for optimality at each step but the final product may be sub-optimal [19].

B. Optimization-based approaches

The GMR can be naturally formulated as an optimization problem [14, 26]. Let S_{OO} , S_{OR} , and S_{RR} be matrices of sizes $N \times N$, $N \times M$, and $M \times M$ with their (n, m) th elements respectively being $\phi(\mu_n; \mu_m, \Sigma_n + \Sigma_m)$, $\phi(\mu_n; \tilde{\mu}_m, \Sigma_n + \tilde{\Sigma}_m)$, and $\phi(\tilde{\mu}_n; \tilde{\mu}_m, \tilde{\Sigma}_n + \tilde{\Sigma}_m)$. Let $w = (w_1, \dots, w_N)^\top$ and $\tilde{w} = (\tilde{w}_1, \dots, \tilde{w}_M)^\top$. Denote by $\Phi(x; G)$ and $\Phi(x; \tilde{G})$ respectively the original and reduced Gaussian mixtures of proper orders. The integrated squared difference between $\Phi(x; G)$ and $\Phi(x; \tilde{G})$ has the following convenient expression [26]:

$$D_{\text{ISE}}(\Phi(\cdot; G), \Phi(\cdot; \tilde{G})) = \int \{\phi(x; G) - \phi(x; \tilde{G})\}^2 dx = w^\top S_{OO} w - 2w^\top S_{OR} \tilde{w} + \tilde{w}^\top S_{RR} \tilde{w}. \quad (2)$$

One optimization-based GMR approach [26] is to search for

$$\tilde{G} := \arg \min \{D_{\text{ISE}}(\Phi(\cdot; G), \Phi(\cdot; \tilde{G})) : \tilde{G} \in \mathbb{G}_M\} \quad (3)$$

where

$$\mathbb{G}_N = \left\{ \sum_{n=1}^N w_n \delta_{\theta_n} : \theta_n \in \Theta, \theta_n \neq \theta_{n'}, w_n > 0, \sum_{n=1}^N w_n = 1 \right\}.$$

Evaluating $D_{\text{ISE}}(\cdot, \cdot)$ is numerically simple but its optimization is expensive. The Quasi-Newton algorithm employed by [26] optimizes over $\mathcal{O}(Md^2)$ variables with the per iteration computational cost at order $\mathcal{O}(NMd^3 + M^2d^4)$. Being quartic in dimension d and quadratic in M , such computational cost becomes unaffordable as d and M increase. Because $D_{\text{ISE}}(\cdot, \cdot)$ is non-convex, the Quasi-Newton algorithm can be trapped at a local minimum. Searching for an algorithm that is less prone to local minima is an important research problem [14].

C. Clustering-based approaches

Both the greedy algorithm-based and optimization-based GMR approaches do not scale when M and d are large. Clustering-based approaches are introduced as their competitors with an advantage in computational efficiency. The clustering-based approaches such as the one in [19] mimic the k -means algorithm [22] in the vector space. They start with a user-proposed M Gaussian distributions as initial cluster centers and iterate between the following two steps:

- *Assignment step*: partition N components of the original mixture into M groups based on their closeness to the current cluster centers according to some divergence $D(\cdot, \cdot)$;
- *Update step*: relocate the cluster centers based on the components assigned to each cluster.

The approach iterates until there are no meaningful changes in these centers. These cluster centers are then exported as M components of the reduced mixture. The mixing weight of each reduced component is the sum of the weights of the original components assigned to the corresponding cluster.

Like the k -means algorithm in the vector space, there can be many assignment schemes. If one assigns each component in the original mixture wholly to a single cluster, the approach is *hard* clustering-based. If one assigns a component of the original mixture in some proportions to more than one cluster, then the approach is *soft* clustering-based. Some existing hard and soft clustering-based approaches for GMR are as follows.

1) *Hard clustering*: In the assignment step, [16], [17], and [19] choose the Kullback–Leibler (KL) divergence as their closeness metric:

$$D_{\text{KL}}(\Phi(\cdot; \theta_n) \| \Phi(\cdot; \tilde{\theta}_m)) = -\log \phi(\mu_n; \tilde{\theta}_m) - \frac{1}{2} \{ \log \det(\Sigma_n) - \text{tr}(\tilde{\Sigma}_m^{-1} \Sigma_n) + C \} \quad (4)$$

where C is a constant that does not depend on any parameters. [18] chooses squared Wasserstein distance [27]

$$W_2^2(\Phi(\cdot; \theta_n) \| \Phi(\cdot; \tilde{\theta}_m)) = \|\mu_n - \tilde{\mu}_m\|^2 + \text{tr}(\Sigma_n + \tilde{\Sigma}_m - 2(\Sigma_n^{1/2} \tilde{\Sigma}_m \Sigma_n^{1/2})^{1/2})$$

as the closeness metric, where $\|\cdot\|$ is the Euclidean norm.

They assign the n th component in the original mixture to the m th cluster when $D(\Phi_n, \tilde{\Phi}_m) = \min_k D(\Phi_n, \tilde{\Phi}_k)$. One may randomly pick one cluster if a component is equally close to more than one cluster. Denote $\mathcal{C}(m)$ the index set of components assigned to the m th cluster in one iteration. Let $\tilde{w}_m = \sum_{n \in \mathcal{C}(m)} w_n$. [19] updates the m th cluster center by moment matching

$$\begin{aligned} \tilde{\mu}_m &= \tilde{w}_m^{-1} \sum_{n \in \mathcal{C}(m)} w_n \mu_n, \\ \tilde{\Sigma}_m &= \tilde{w}_m^{-1} \sum_{n \in \mathcal{C}(m)} w_n \{ \Sigma_n + (\mu_n - \tilde{\mu}_m)(\mu_n - \tilde{\mu}_m)^\top \}. \end{aligned} \quad (5)$$

[18] updates by the Wasserstein barycenter of $\{\phi(x; \theta_n) : n \in \mathcal{C}(m)\}$. The iteration continues until the change in the integrated squared error $D_{\text{ISE}}(\Phi(\cdot; G), \Phi(\cdot; \tilde{G}))$ is below some user-specified threshold.

2) *Soft clustering*: Instead of assigning the whole component of the original mixture to a single cluster, the soft clustering-based approach assigns z_{nm} fraction of the n th component to the m th cluster for some $z_{nm} \geq 0$ and $\sum_{m=1}^M z_{nm} = 1$. Various forms of z_{nm} have been considered in the literature. For instance, [15] let $z_{nm} \propto \tilde{w}_m \exp(w_n I E_{nm})$ and [10] uses $z_{nm} \propto \tilde{w}_m \exp(I E_{nm})$ with some hyper-parameter $I > 0$ and $E_{nm} = \int \phi(x; \theta_n) \log \phi(x; \tilde{\theta}_m) dx$. They also use moment matching to update the cluster centers.

The soft clustering-based approach reduces to the hard clustering-based approach as the hyper-parameter $I \rightarrow \infty$. This is seen by noticing

$$z_{nm} = \frac{\tilde{w}_m \exp(I E_{nm})}{\sum_k \tilde{w}_k \exp(I E_{nk})} = \left\{ 1 + \sum_{k \neq n} \frac{\tilde{w}_k \exp(I E_{nk})}{\tilde{w}_m \exp(I E_{nm})} \right\}^{-1} \rightarrow 1$$

when $E_{nm} = \max_k E_{nk}$ and 0 otherwise as $I \rightarrow \infty$. The computational cost of both hard and soft clustering-based algorithms is $\mathcal{O}(NMd^3)$ at each iteration, which is lower than the per iteration cost of the optimization-based approach in [13].

III. PROPOSED GAUSSIAN MIXTURE REDUCTION METHOD

We formulate the GMR problem as an optimization problem. One of many key ingredients of our proposed GMR method is the use of composite transportation divergence. Most divergences are computationally difficult between two Gaussian mixtures but easy between two Gaussian distributions. To leverage this computational efficiency, we view Gaussian mixtures as discrete distributions on the space of Gaussian distributions. We then endow the space of the Gaussian distributions with carefully selected divergence to define an easy-to-compute composite transportation divergence between finite Gaussian mixtures.

We give the definition of the divergence, the problem formulation, and the proposed numerical algorithm in the rest of this section.

A. Composite transportation divergence

Denote by $\Phi(x; G)$ and $\Phi(x; \tilde{G})$ respectively the original and reduced Gaussian mixtures of proper orders. We denote their corresponding mixing weights by w and \tilde{w} , and components by Φ_n and $\tilde{\Phi}_m$. We define the composite transportation divergence (CTD) from the original to the reduced mixture as follows.

Definition 1 (Composite transportation divergence). *Let $c(\cdot, \cdot)$ be a divergence on the space of Gaussian distributions, $\mathcal{F} = \{\phi(\cdot; \mu, \Sigma)\}$. The composite transportation divergence [24, 28] between two finite Gaussian mixtures with cost function $c(\cdot, \cdot)$ is*

$$\mathcal{T}_c(\Phi(\cdot; G), \Phi(\cdot; \tilde{G})) = \inf_{\pi \in \Pi(w, \tilde{w})} \left\{ \sum_{n,m} \pi_{nm} c(\Phi_n, \tilde{\Phi}_m) \right\}$$

where

$$\Pi(w, \tilde{w}) = \left\{ \pi \in \mathbb{R}_+^{N \times M} : \sum_{n=1}^N \pi_{nm} = \tilde{w}_m, \sum_{m=1}^M \pi_{nm} = w_n \right\}.$$

Let $\lambda \geq 0$ be a regularization parameter. An entropy regularized composite transportation divergence is

$$\mathcal{T}_c^\lambda(\Phi(\cdot; G), \Phi(\cdot; \tilde{G})) = \inf_{\pi \in \Pi(w, \tilde{w})} \left\{ \sum_{n,m} \pi_{nm} c(\Phi_n, \tilde{\Phi}_m) - \lambda \mathcal{H}(\pi) \right\} \quad (6)$$

with entropy $\mathcal{H}(\pi) = -\sum_{n,m} \pi_{nm} (\log \pi_{nm} - 1)$.

The entropy regularized CTD reduces to the CTD when $\lambda = 0$. We write $\mathcal{T}_c^\lambda(\tilde{G}) = \mathcal{T}_c^\lambda(\Phi(\cdot; G), \Phi(\cdot; \tilde{G}))$ for brevity when appropriate.

The CTD between two mixtures can be view as the optimal transport divergence [29] between two mixing distributions G and \tilde{G} . The optimal transport divergence is a byproduct of the optimal transportation problem and there is a canonical example to explain the intuition behind the divergence. Suppose an operator runs N warehouses and M factories in the space of Gaussian distributions \mathcal{F} . The n th warehouse at location Φ_n contains w_n units of raw material and the m th factory at location $\tilde{\Phi}_m$ requires \tilde{w}_m units of raw material. Let $c(\Phi_n, \tilde{\Phi}_m)$ be the unit cost to transport materials from warehouse n to factory m and $\pi_{nm} \geq 0$ be the amount of material being transported. Suppose the cost is proportional to the amount of material to be transported, then $\sum_{n,m} \pi_{nm} c(\Phi_n, \tilde{\Phi}_m)$ is the total transportation cost under the transportation plan π . The set $\Pi(w, \tilde{w})$ is all possible transportation plans which must satisfy two marginal constraints: (a) the right amount of materials are taken from warehouses, and (b) the right amount of materials is received by factories. The optimal transportation problem seeks the optimal transportation plan π^* that leads to the lowest total cost among all feasible plans in $\Pi(w, \tilde{w})$. The lowest total cost under the optimal transportation plan then becomes the CTD between two mixtures. The optimal transportation plan is usually computed with numerical algorithms such as linear programming and the computational cost is $\mathcal{O}(N^3 \log N)$ when $N = M$. The computational cost increases as N increase and the entropic regularized version of the optimal transportation problem was proposed to lower the computational cost. In our GMR problem, however, the entropic regularized CTD serves a different purpose as we will explained in Section III-D.

B. Proposed approach

Given a cost function $c(\cdot, \cdot)$ on the space of Gaussian distributions and a regularization parameter $\lambda \geq 0$, we propose to reduce $\Phi(\cdot; G)$ of order N to $\Phi(\cdot; \tilde{G})$ of order M with

$$\tilde{G} = \arg \inf \{ \mathcal{T}_c^\lambda(G^\dagger) : G^\dagger \in \mathbb{G}_M \}. \quad (7)$$

Our approach belongs to the optimization category and it has two apparent advantages:

- First, the evaluation of the objective function is decomposed into easy-to-evaluate divergences between component distributions.
- Second, the composite structure also permits an easy-to-implement numerical algorithm.

At the first glance, searching for \tilde{G} in (7) must solve two subproblems both involve a constrained optimization issue: (1) evaluating $\mathcal{T}_c^\lambda(G^\dagger)$ for each G^\dagger ; (2) minimizing $\mathcal{T}_c^\lambda(G^\dagger)$ with respect to G^\dagger . The first subproblem necessitates numerical searching of transportation plans π with w and \tilde{w} to be its two marginal measures. In fact, this is not necessary and two subproblems can be seamlessly solved by a single MM algorithm. The intuition is as follows.

Recall that the CTD is the lowest cost of transporting material from warehouses to factories. The optimal π transports warehouse subpopulations to the factory subpopulations at the lowest cost. Transporting all materials in warehouses to factories necessitates π to have the first marginal matching the warehouse mixing distribution and the second marginal matching the factory mixing distribution. In the context of our GMR approach, however, the factory mixing distribution is a subject being optimized. We can therefore take whatever the second marginal of π is, rather than impose a form on it. In other words, instead of choosing π to have \tilde{w} as its second marginal, we let \tilde{w} be the second marginal of π . This makes the marginal distribution constraint \tilde{w} on π redundant. After removing this redundant constraint, the optimal transportation plan with one marginal constraint has a closed-form and allows an easy-to-implement majorization-minimization (MM) algorithm. We give the algorithm based on this insight formally in the next section.

C. The tailor-made MM algorithm

We now present the tailor-made MM algorithm for (7). Let $\Pi(w, \cdot) = \{ \pi \in \mathbb{R}_+^{N \times M} : \sum_{m=1}^M \pi_{nm} = w_n \}$. Define two functions with their dependency on the original G hidden:

$$\mathcal{J}_c^\lambda(G^\dagger) = \inf_{\pi \in \Pi(w, \cdot)} \left\{ \sum_{n,m} \pi_{nm} c(\Phi_n, \Phi_m^\dagger) - \lambda \mathcal{H}(\pi) \right\}, \quad (8)$$

$$\pi^\lambda(G^\dagger) = \arg \inf_{\pi \in \Pi(w, \cdot)} \left\{ \sum_{n,m} \pi_{nm} c(\Phi_n, \Phi_m^\dagger) - \lambda \mathcal{H}(\pi) \right\}. \quad (9)$$

The optimization operations in (8) and (9) involve only one linear marginal constraint in terms of w . Once the target component Gaussian distributions Φ_m^\dagger are given, the optimal transportation plan $\pi^\lambda(G^\dagger)$ has its (n, m) th entry:

$$\pi_{nm}^\lambda(G^\dagger) = \frac{w_n \exp\{-c(\Phi_n, \Phi_m^\dagger)/\lambda\}}{\sum_k \exp\{-c(\Phi_n, \Phi_k^\dagger)/\lambda\}}. \quad (10)$$

When $\lambda = 0$, the solution is given by $\pi_{nm}^0(G^\dagger) = \lim_{\lambda \downarrow 0} \pi_{nm}^\lambda(G^\dagger)$.

Theorem 1 (Equivalent optimization problem with single marginal constraint). *Let G , $\mathcal{T}_c^\lambda(\cdot)$, $\mathcal{J}_c^\lambda(\cdot)$, $\pi^\lambda(\cdot)$, and the other notation be the same as given earlier. We have*

$$\inf \{ \mathcal{T}_c^\lambda(G^\dagger) : G^\dagger \in \mathbb{G}_M \} = \inf \{ \mathcal{J}_c^\lambda(G^\dagger) : G^\dagger \in \mathbb{G}_M \}.$$

The reduced mixture hence is $\tilde{G} = \arg \inf \{ \mathcal{J}_c^\lambda(G^\dagger) : G^\dagger \in \mathbb{G}_M \}$ with mixing weight of the m th component being $\tilde{w}_m = \sum_n \pi_{nm}^\lambda(\tilde{G})$.

The proof is given in Appendix A. We develop an iterative procedure following the well-known MM algorithm [30]. For completeness, we provide a brief overview of the MM algorithm following [30]. Suppose we wish to minimize a function $g(x)$ over some space \mathcal{X} . The MM algorithm iteratively updates a solution from an initial point $x_0 \in \mathcal{X}$. After t iterations, with the current solution x_t , MM algorithm first constructs a function $h(x|x_t)$ that majorizes $g(x)$ at x_t , that is $h(x|x_t) \geq g(x)$ with equality holds at $x = x_t$. It then updates x_t with $x_{t+1} = \arg \min \{ h(x|x_t) : x \in \mathcal{X} \}$. The success of MM algorithm relies on finding a majorization function $h(x|x_t)$, preferably convex in x , that is easy to minimize. Such a procedure ensures a decreasing sequence of $g(x_t)$.

We now present the majorization and minimization steps in minimizing (8).

Majorization Let $\tilde{G}^{(t)}$ be the mixing distribution updated after t iterations. We first propose a majorization function for the optimization goal (8):

$$\mathcal{K}_c^\lambda(G^\dagger | \tilde{G}^{(t)}) = \sum_{n,m} \pi_{nm}^\lambda(\tilde{G}^{(t)}) c(\Phi_n, \Phi_m^\dagger) - \lambda \mathcal{H}(\pi^\lambda(\tilde{G}^{(t)})) \quad (11)$$

with $\pi_{nm}^\lambda(\tilde{G}^{(t)})$ dependent on the entropy regularization strength λ as in (10).

Minimization We then minimize the majorization function (11) and update Φ_m^\dagger for each m :

$$\tilde{\Phi}_m^{(t+1)} = \arg \inf_{\Phi^\dagger \in \mathcal{F}} \left\{ \sum_n \pi_{nm}^\lambda(\tilde{G}^{(t)}) c(\Phi_n, \Phi^\dagger) \right\} \quad (12)$$

where \mathcal{F} is the family of d -dimensional Gaussian distributions.

The new minimizing problem in (12) is simpler than directly solving (8). Because the parameters Φ_m^\dagger in G^\dagger are separated in the majorization function (11) by design, we can optimize with respect to Φ_m^\dagger separately and in parallel.

The proposed algorithm is also helped by the fact that we can update the mixing proportions $\tilde{w}_m^{(t)}$ and the subpopulation parameters $\tilde{\Phi}_m^{(t)}$ in sequence. We first let

$$\tilde{w}_m^{(t+1)} = \sum_n \pi_{nm}^\lambda(G^{(t)})$$

and then obtain $\tilde{\Phi}_m^{(t+1)}$. The algorithm then iterates between the majorization step (11) and the minimization step (12) until the reduction in $\mathcal{J}_c^\lambda(\tilde{G}^{(t)})$ is below some threshold. The algorithm can be summarized by Algorithm 1.

Algorithm 1 MM algorithm for GMR with CTD

Initialization: $\tilde{\Phi}_m, m \in [M]$

repeat

for $m \in [M]$ **do**

Majorization: compute π_{nm}^λ according to (10).

Minimization:

 Let $\tilde{\Phi}_m = \arg \min_{\Phi} \sum_n \pi_{nm}^\lambda c(\Phi_n, \Phi)$

 Let $\tilde{w}_m = \sum_n \pi_{nm}^\lambda$

end for

until $\sum_{n,m} \pi_{nm}^\lambda c(\Phi_n, \tilde{\Phi}_m) - \lambda \mathcal{H}(\pi^\lambda)$ converges

The following theorem asserts that the algorithm converges under some conditions.

Theorem 2. Suppose the cost function $c(\cdot, \cdot)$ is continuous in both arguments. Assume that for any constant $\Delta > 0$ and $\Phi^* \in \mathcal{F}$, the following set is compact according to some distance on \mathcal{F} :

$$\{\Phi : c(\Phi^*, \Phi) \leq \Delta\}.$$

Let $\{\tilde{G}^{(t)}\}$ be the sequence of mixing distributions generated by $\tilde{G}^{(t+1)} = \arg \min \mathcal{K}_c(G^\dagger | \tilde{G}^{(t)})$ with some initial mixing distribution $\tilde{G}^{(0)}$. Then

- 1) $\mathcal{J}_c^\lambda(\tilde{G}^{(t+1)}) \leq \mathcal{J}_c^\lambda(\tilde{G}^{(t)})$ for any t ;
- 2) if G^* is a limiting point of $\tilde{G}^{(t)}$, then $\tilde{G}^{(t)} = \tilde{G}^*$ implies $\mathcal{J}_c^\lambda(\tilde{G}^{(t+1)}) = \mathcal{J}_c^\lambda(\tilde{G}^*)$.

In addition, the algorithm will attain at least a local optimal solution after a finite number of iterations when $\lambda = 0$.

The proof is in the supplementary material. The first two properties in this theory imply that $\mathcal{J}_c^\lambda(\tilde{G}^{(t)})$ converges monotonically to some constant J^* . All limiting points $\tilde{G}^{(t)}$ are stationary points of $\mathcal{J}_c^\lambda(\cdot)$: iterations from \tilde{G}^* do not further reduce the value of $\mathcal{J}_c^\lambda(\cdot)$. When $\lambda = 0$, the upper bound for the number of iterations is M^N . In theory, one can exhaust M^N situations to find the global optimal solution. See the explanations in the supplementary material. We are short of proving if a similar conclusion holds when $\lambda > 0$.

One primary advantage of our proposed approach for GMR compared with other optimization-based approaches is this easy-to-implement algorithm and its computational efficiency. In the assignment step, the optimal transportation has a closed-form and can be computed at cost $\mathcal{O}(NM)$ given $c(\cdot, \cdot)$ values. The per evaluation cost of commonly used $c(\cdot, \cdot)$ is $\mathcal{O}(d^3)$. Therefore, the total cost for the assignment step is $\mathcal{O}(NMd^3)$. The updating step (12) solves for barycenter [31] for M clusters with costs depending on the cost function employed in the CTD in (6). When the cost function is KL divergence, the corresponding Gaussian barycenter can be computed at cost $\mathcal{O}(d^2)$. The per iteration cost in this case is $\mathcal{O}(NMd^3)$, which is lower than the per iteration cost of directly minimizing the integrated squared error in Section II that is quartic in d .

D. Generality of the proposed approach

It is demonstrated in [19] that the hard clustering-based approaches are in general computationally cheaper than directly minimizing the integrated squared distance. They also beat some greedy algorithms such as [25] and [12]. However, the convergence of hard clustering-based approaches and their optimality were not previously studied. In this section, we show our proposed approach unifies existing clustering-based approaches. Our proposed MM algorithm leads to both hard or soft clustering-based Gaussian mixture reduction methods when $\lambda = 0$ or $\lambda > 0$ respectively. Consequently, we succeed in

theoretically proving the optimality objective of existing cluster-based methods. In addition, our Theorem 2 also establishes their algorithm convergence.

Suppose we choose $\lambda = 0$ and let the cost function be the KL divergence $c(\Phi_n, \tilde{\Phi}_m) = D_{\text{KL}}(\Phi_n \| \tilde{\Phi}_m)$. Let $\tilde{\Phi}_m^{(t)}$ be the cluster center after t iterations. For the ease of presentation, suppose for every n , $n' = \arg \min_m D_{\text{KL}}(\Phi_n \| \tilde{\Phi}_m^{(t)})$ is unique. In this case, the transportation plan in the MM algorithm is

$$\tilde{\pi}_{nm}^{(t+1)} = \begin{cases} w_n & \text{when } m = n', \\ 0 & \text{otherwise.} \end{cases}$$

The mixing weight of $\tilde{\Phi}_m^{(t+1)}$ is $\tilde{w}_m = \sum_{n=1}^N \tilde{\pi}_{nm}^{(t+1)}$ with

$$\tilde{\Phi}_m^{(t+1)} = \arg \inf \left\{ \sum_{n=1}^N \tilde{\pi}_{nm}^{(t+1)} D_{\text{KL}}(\Phi_n \| \Phi^\dagger) : \Phi^\dagger \in \mathcal{F} \right\}$$

which is the KL barycenter. As will be shown in supplementary material, the barycenter solution coincides with moment matching solution for Gaussian mixture. Hence, the proposed GMR approach with $\lambda = 0$ and KL divergence as cost function leads to the hard-clustering GMR algorithm in [19]. Similarly, let $\lambda = 0$ and $c(\Phi_n, \tilde{\Phi}_m)$ be the 2-Wasserstein distance $W_2(\Phi_n, \tilde{\Phi}_m)$ between two Gaussians, the proposed GMR leads to the hard-clustering algorithm in [18].

Let $\lambda = 1$ and $c(\Phi_n, \tilde{\Phi}_m) = -\log \tilde{w}_m + ID_{\text{KL}}(\Phi_n \| \tilde{\Phi}_m)$. Our proposed algorithm reduces to the soft clustering-based algorithm of [10]. Regretfully, this cost function depends on the mixing weights of the reduced mixture. Hence, Theorem 2 does not directly apply and its convergence remains unclear. Yet we provide a valid motivation for this algorithm.

The soft-clustering algorithm in [10] is motivated by the variational inference [32]. Suppose we have I random observations from $\Phi(x; G)$. Let the data be $X = (X_1, X_2, \dots, X_I)^\top$ so that the log-likelihood function is $\sum \log \phi(X_i; \tilde{G})$. Its expectation is

$$\ell_I(\tilde{G}) = E \left\{ \sum_{i=1}^I \log \phi(X_i; \tilde{G}) \right\} = IE \{ \log \phi(X_1; \tilde{G}) \}.$$

Let Y_{n1}, \dots, Y_{nI} be a random sample from $\Phi(y; \theta_n)$ for each n . It appears that [10] suggests

$$\ell_I(\tilde{G}) = \sum_{n=1}^N w_n E \left\{ \sum_{i=1}^I \log \phi(Y_{ni}; \tilde{G}) \right\}.$$

Conceptually, this claim amounts to regarding X to have a probability w_n to be a random sample from the subpopulation $\phi(y; \theta_n)$. This is not true and invalidates the suggested variational lower bound.

IV. EXPERIMENTS

A. General experimental setting

We demonstrate the effectiveness of the proposed GMR approach through experiments. We experiment with cost functions in the CTD being the integrated squared error

$$D_{\text{ISE}}(\Phi_n, \tilde{\Phi}_m) = \phi(\mu_n; \mu_n, 2\Sigma_n) + \phi(\tilde{\mu}_m; \tilde{\mu}_m, 2\tilde{\Sigma}_m) - 2\phi(\mu_n; \tilde{\phi}_m, \Sigma_n + \tilde{\Sigma}_m) \quad (13)$$

and the KL divergence in (4). We refer to the resulting methods or outcomes as CTD-ISE and CTD-KL. We also include the optimization-based reduction method of [26] as the baseline for comparison and the method is named as ISE as in (3). With KL divergence, the proposed GMR approach reduces to the existing clustering-based approach.

The regularization parameter λ plays an important role in the quality of reduction. We experiment on different levels of regularization to cover both hard and soft clustering-based algorithms. For a given cost function of the CTD in the proposed approach, we use the λ value that achieves the lowest integrated square error between the original and reduced mixtures over a grid of λ values. We initialize all algorithms with 10 multiple initial values to avoid local minimum. The stopping criterion for the algorithm is that the change in the objective function is below 10^{-8} . We compare the average run time of the algorithms over multiple initializations. We implement experiments in Python 3.7.4 on the Narval cluster at Compute Canada. The codes are publicly available at <https://github.com/SarahQiong/CTDGMR>.

B. Simulated mixtures

We first consider reducing a bivariate Gaussian mixture of order $N = 25$. Rather than selecting original mixtures arbitrarily, we generate $R = 100$ of them with some structure at random. We generate the parameter values of the original mixture in each repetition as follows.

We let all subpopulations have equal mixing weight with $w_j = 0.04$ for all $j = 1, \dots, 25$. We generate a multinomial random vector $(n_1, \dots, n_5)^\top$ with equal event probability and choose μ_i uniformly and randomly from $[-10, 10] \times [-10, 10]$. We then

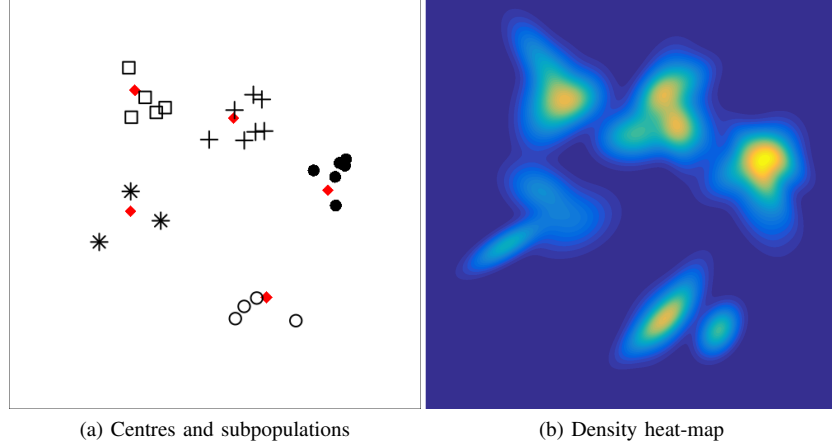


Fig. 2: A typical order $N = 25$ original Gaussian mixture. (a) Centres marked as diamonds and locations of subpopulation means. (b) Heat map of the density function of the original mixture.

generate μ_{ij} uniformly in the circle with radius 2.5 and let the subpopulation means be $\{\mu_i + \mu_{ij}, j = 1, \dots, n_i, i = 1, \dots, 5\}$. The resulting subpopulations are roughly clustered around 5 random centers. See Fig. 2 (a) for a typical outcome.

We next generate $N = 25$ subpopulation covariance matrices. We first generate $\sigma_{11n}, \sigma_{22n}$ independently from Gamma distribution with shape parameter 8 and scale parameter 4 followed by a rotation angle β_n uniformly in $[36^\circ, 144^\circ]$. We then let

$$\Sigma_n = \begin{pmatrix} \sigma_{11n} & \sqrt{\sigma_{11n}\sigma_{22n}} \cos(\beta_n) \\ \sqrt{\sigma_{11n}\sigma_{22n}} \cos(\beta_n) & \sigma_{22n} \end{pmatrix}$$

be the n th subpopulation covariance matrix. Fig. 2 (b) shows the heat map of a typical density function. This design ensures the reduction is a meaningful exercise and there is enough uncertainty to set apart various reduction methods.

Given the knowledge of how the original mixtures are generated, it is natural to reduce the original mixture to order $M = 5$. In real-world applications, we most likely do not have such knowledge. Therefore, we experiment with M ranging from 3 to 22.

We apply three reduction methods listed in Section IV-A to each randomly created original mixture. We provide the integrated squared error in (2) between the original and reduced mixtures, which serves as a performance measure. The lower the value, the better the performance. For soft clustering algorithms, we search over $\lambda = 0.001, 0.005, 0.01, 0.05, 0.1, 0.15$, and 0.2 for each randomly created mixture and report the lowest integrated squared error. Fig. 4 shows their performances in terms of approximation precision and computational time. We also experimented on higher dimension Gaussian mixtures. Due to space limits, we do not present these results and these methods have similar relative performances.

All three reduction methods have improved reduction performance and take more time to compute as M increases. They all lead to satisfactory reduction outcomes. By definition, the ISE approach of [26] achieves the smallest integrated squared error. The simulation results show that the proposed CTD-based methods, CTD-ISE and CTD-KL, attain similar precision when $M = 5$ or slightly worse with meaningful reduction results. Most importantly, these are achieved at much lower computational costs. The precision comparison is not as favorable when $M > 10$ but the proposed methods are more favorable in terms of computational time. For example, when $M = 22$, the [26] approach uses 1000 folds computation time as the proposed approach with KL divergence as the cost function. The proposed approach with cost function (13) has comparable precision to the [26] approach while using only 1/10th computation time. Soft clustering methods outperform their hard clustering counterparts in precision with slightly more computational time as they take more iterations to converge. In summary, the proposed approach leads to mixture reduction methods that achieve satisfactory precision with much lower computational cost.

C. Approximate inference in belief propagation

This experiment illustrates the effectiveness of Gaussian mixture reduction in belief propagation. The belief propagation is an iterative algorithm used to compute the marginal distributions in the graphical model. Specifically, let there be a graph with a node set \mathcal{V} and an undirected edge set \mathcal{E} . A probabilistic graphical model associates each node with a random variable, say X_i , and postulates that the density function of the random vector $X = \{X_i : i \in \mathcal{V}\}$ can be factorised into

$$p(x) \propto \prod_{(i,j) \in \mathcal{E}} \psi_{ij}(x_i, x_j) \prod_{i \in \mathcal{V}} \psi_i(x_i)$$

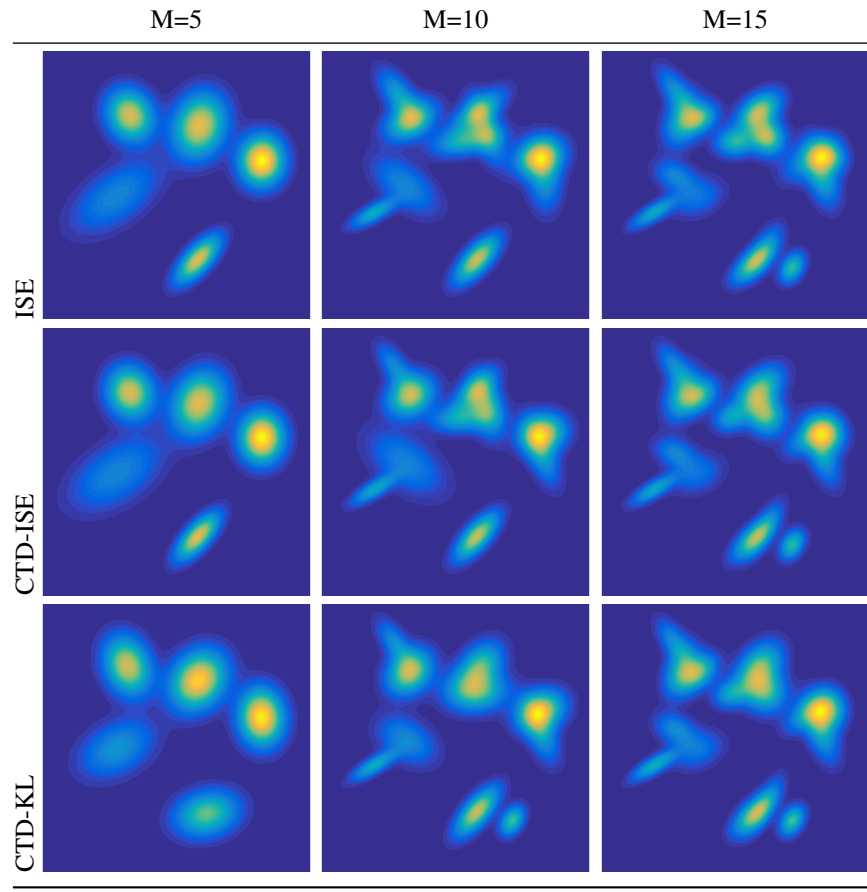


Fig. 3: Heat maps of the density functions of the reduced mixture.

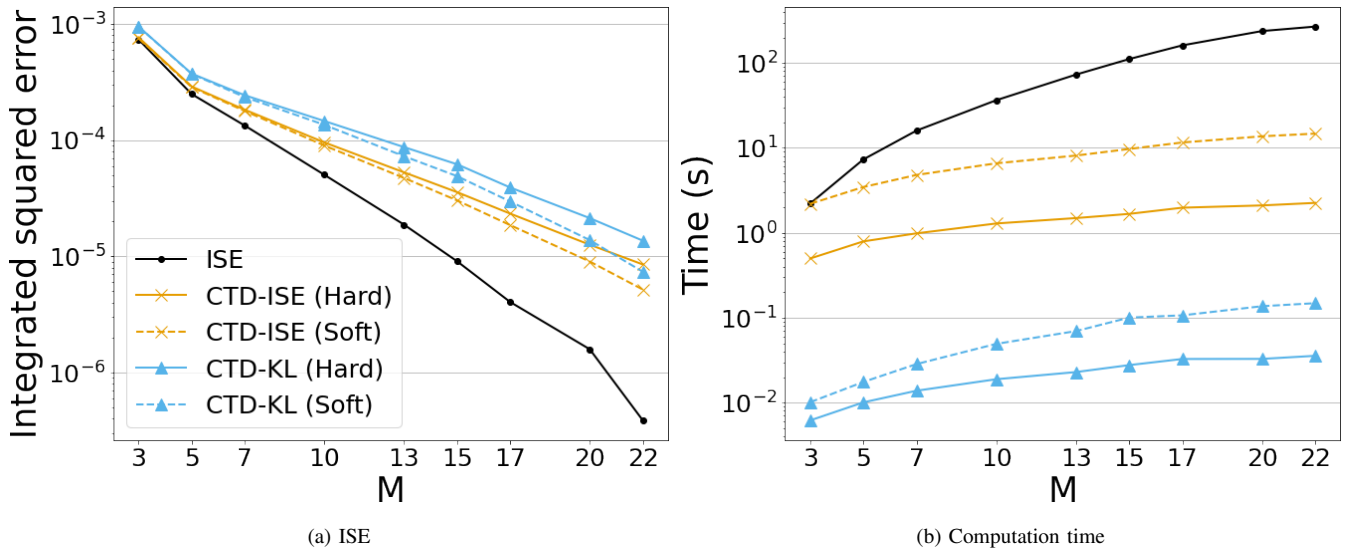


Fig. 4: (a) D_{ISE} between the reduced and original mixtures. (b) The computation time. The plot includes the reduction approaches MISE (solid line with dot), hard CTD-KL (solid line with triangle), soft CTD-KL (dashed line with triangle), hard CTD-ISE (solid line with cross), and soft CTD-ISE (dashed line with cross).

for some non-negative valued functions $\psi_{ij}(\cdot, \cdot)$ and $\psi_i(\cdot)$. We call $\psi_{ij}(\cdot, \cdot)$ local potential and $\psi_i(\cdot)$ local evidence potential. Denote the neighbourhood of a node i as $\Gamma(i) := \{j : (i, j) \in \mathcal{E}\}$. A message $m_{ji}(\cdot)$ is a function associated with edge (i, j) and it is updated in the t th step according to

$$m_{ji}^{(t)}(x_i) \propto \int \psi_{ij}(x_i, x_j) \psi_j(x_j) \prod_{k \in \Gamma(j) \setminus i} m_{kj}^{(t-1)}(x) dx. \quad (14)$$

The belief function $q_i(\cdot)$ associated with the density function of X_i is updated in the t th step according to

$$q_i^{(t)}(x) \propto \psi_i(x) \prod_{j \in \Gamma(i)} m_{ji}^{(t)}(x). \quad (15)$$

The messages and beliefs are iteratively updated until convergence. We refer to the above procedure as belief propagation.

In belief propagation, the closed-form outcome of the messages generally does not exist. To ensure efficient inference, density functions of Gaussian mixtures are often used to approximate the messages for two reasons. First, they are flexible to approximate any density function to arbitrary precision. Second, they lead to closed-form outputs in the message and belief updates, which are also mixtures whose orders increase exponentially as iterations. However, this naive iterative procedure quickly becomes intractable. One remedy is to perform a Gaussian mixture reduction step after each iteration to stop the order from increasing exponentially.

We apply the proposed GMR methods to the belief propagation for the model represented by Fig. 5 (a) following [10]. We let $\psi_{ij}(x, y) = \phi(x; y, \phi_{ij}^{-1})$, with ϕ_{ij} marked alongside the graph edges in the figure and

$$\psi_i(x) = w_i \phi(x; \mu_{i1}, 1) + (1 - w_i) \phi(x; \mu_{i2}, 1.5).$$

We create $R = 100$ graphs with parameter values generated independently and identically distributed according to: $w_i \sim U(0, 1)$, $\mu_{i1} \sim U(-4, 0)$, and $\mu_{i2} \sim U(0, 4)$. We obtain *exact inference* following (14) and (15) for the first 4 iterations and it becomes infeasible for more iterations. We reduce the order of the message mixture to $M = 4$ using three reduction methods after any iteration when its order exceeds 4 following [10]. We then use the reduced message mixture to update the beliefs according to (15) leading to approximated beliefs.

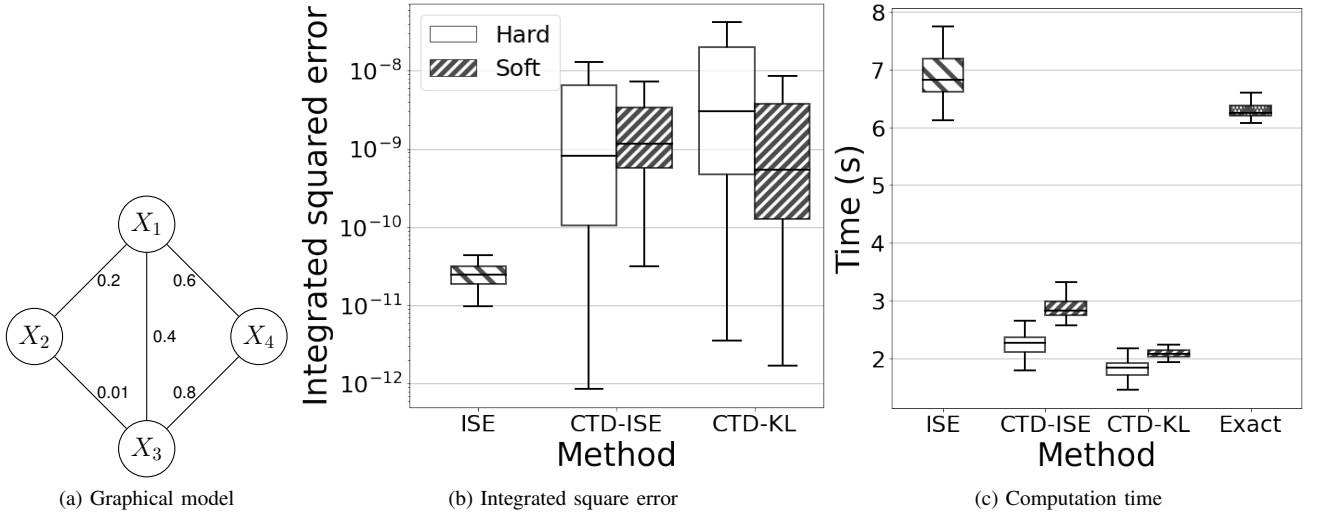


Fig. 5: (a) Graphical model. (b) Integrated squared error between the exact and approximate beliefs. (c) Computation times for belief update. The proposed methods include soft clustering-based (boxes without hatching pattern) and hard clustering-based (diagonal hatching).

We use integrated squared error to evaluate the performance of the reduction methods averaged across 4 nodes and the first 3 iterations. For the soft clustering-based methods, we use λ values over the same grids as Section IV-B. The integrated squared error is computed for each fixed λ value applied to all nodes and in all iterations. That is, the performance is tallied for each λ value, not cherry-picked over repetitions. The reported integrated squared error is the lowest one achieved by a single λ value.

Fig. 5 (b) contains box-plots of 100 outcomes. By definition, the ISE approach has the lowest integrated squared error. As anticipated, both CTD-ISE and CTD-KL do not attain as low integrated squared error as the ISE, but they use much less computation time. Similar to the experiments on the simulated mixtures, the proposed methods corresponding to soft clustering have lower integrated squared error values and use slightly more computation time. They have lower variation with cost function (13) and higher precision with the KL divergence cost function than their hard clustering counterpart.

D. Real data application for hand gesture recognition

Static hand gesture recognition is the task of training a classifier to identify the gesture of future images given a set of labeled images of hand gestures. We use the Jochen Triesch static hand posture database in [33] that is publicly available online. This dataset contains 128×128 greyscale images of 10 hand postures forming the alphabetic letters: A, B, C, D, G, H, I, L, V, and Y by 24 persons with 3 different backgrounds. We use the same set of images as described in [34] to remove the backgrounds. The hands in these images are centered on cropping and subsequently resized. After pre-processing, we have 168 images in total with 16–20 images for each hand posture.

[34] view the intensity of each pixel as a function of the location. They approximate this function by the density function of a Gaussian mixture up to some normalization constant. They fit an order of 10 Gaussian mixture for each image. We give one original image and the heat map of the density function of the corresponding fitted mixture in Fig. 6.

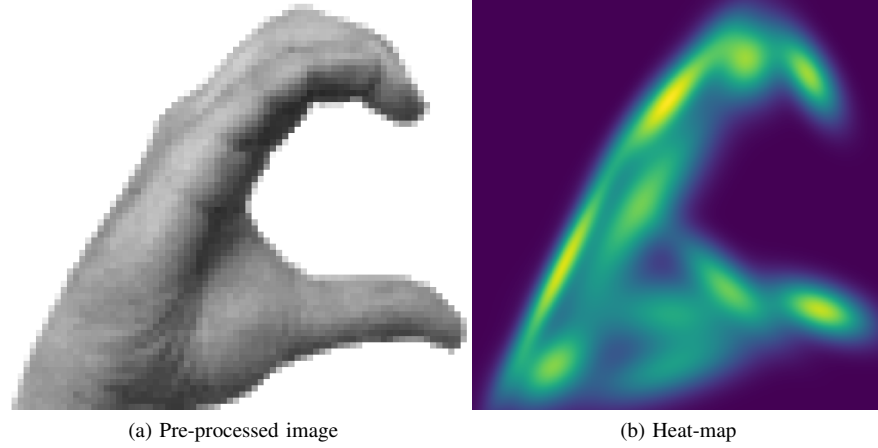


Fig. 6: (a) A typical pre-processed image of hand posture “C”. (b) Heat map of a fitted order 10 Gaussian mixture for the image in (a).

[34] classify a new image based on its Cauchy–Schwarz divergence [35] to all training images. A test image of hand posture is classified as posture “A” if there is a training image with hand posture “A” that is closest to this test image. This approach achieves a cross-validation classification accuracy of 95.2%. When there are many training images, this test procedure can be time-consuming. We investigate if the proposed GMR approach combined with a slightly different strategy from [34] may lead to a competitive alternative.

We first create a representative image for each class and call it a class prototype. Instead of comparing the test image with all training images, we compare it with the class prototypes. When the number of training images is very large, this approach dramatically reduces the number of comparisons, perhaps at some cost in classification accuracy. More specifically, each original training image is first replaced by a mixture followed by combining the training images of the same hand posture into a single mixture. This single mixture is formed by direct summation and has a much higher order. We then reduce the order of the summed-up mixture of each hand posture to order 10 Gaussian mixture to be used as the class prototype. We use the nearest neighbor classifier subsequently. Fig. 7 gives the prototypes of the hand postures we obtained.

Method	A	B	C	D	G	H	I	L	V	Y
ISE										
CTD-KL										
CTD-ISE										

Fig. 7: The class prototypes of hand gestures obtained by different reduction approaches.

We compare the classification accuracy and computation time of various reduction methods. Since the training set is relatively small, we perform 5-fold cross-validation that is repeated 100 times to gauge the classification accuracy. We consider two schemes:

- 1) Use the same divergence for classification and for reduction. For instance, we minimize the integrated squared error to both obtain the class prototype and measure the similarity between the test images and the class prototypes. Fig. 8 (a) depicts the classification accuracy of this strategy using different reduction methods. For the proposed methods based on the soft clustering algorithm, we search over the same λ grid as before and use the same value of λ for each posture and each cross-validation fold.
- 2) We also experiment on different divergences employed for test and for reduction. For example, we may minimize the integrated squared error to obtain the class prototype but use the CTD with KL divergence as the cost function to measure the similarity between the test images and the class prototypes. Fig. 8 (b) depicts the classification accuracy with this strategy based on different combinations of divergences. We only include the proposed approach with $\lambda = 0$ to avoid the excessive number of possible combinations.

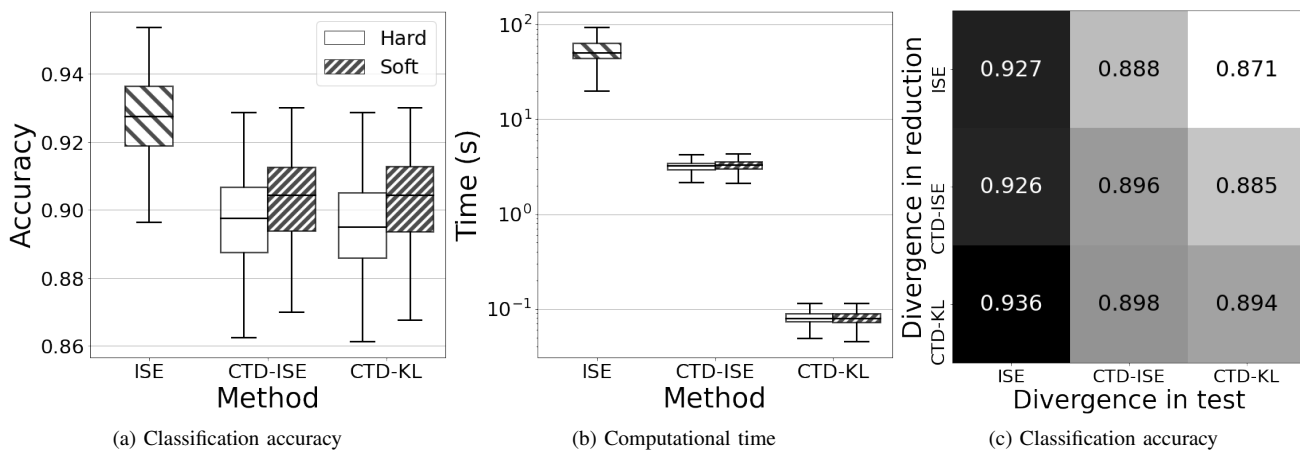


Fig. 8: (a) Classification accuracy when the reduction and test use the same divergence. (b) Computational time of different reduction approaches. (c) Classification accuracy when the reduction and test use the different divergences. The proposed methods include soft clustering-based (boxes without hatching pattern) and hard clustering-based (diagonal hatching).

When the same divergence is used in reduction and test, the ISE achieves the highest classification accuracy. However, it requires more computation time. Our proposed methods have slightly lower classification accuracy but the computation time was greatly reduced. Our proposed soft clustering-based approach also leads to higher accuracy. When different divergences are used in reduction and test, the accuracy is best using integrated squared error for the test. All reduction methods have satisfactory classification accuracy. Overall, using CTD-KL for reduction and CTD-ISE for testing is the best combination for both computation time and classification accuracy.

V. CONCLUSION

In this paper, we propose a novel Gaussian mixture reduction approach and an iterative algorithm with proven convergence properties. The proposed method includes many existing clustering-based methods as special cases. We demonstrate the effectiveness of the proposed approach with numerical experiments on simulated and real datasets. This paper only includes experiment results of the proposed approach with integrated squared error and KL as cost functions in the first two experiments and excludes results based on other cost functions to save space. The user can certainly use the most appropriate cost functions in their applications. We present theoretical derivations in the supplementary material.

APPENDIX A
PROOF OF THEOREM 1

Proof. The key conclusion of this theorem is

$$\inf\{\mathcal{T}_c^\lambda(G_M) : G_M \in \mathbb{G}_M\} = \inf\{\mathcal{J}_c^\lambda(G_M) : G_M \in \mathbb{G}_M\}$$

under the constraint that the mixing weights of the optimal mixing distribution of the right-hand-side are

$$\tilde{w}_m = \sum_{n=1}^N \pi_{nm}^\lambda(G_M), \quad \forall m = 1, 2, \dots, M.$$

We prove this result by showing both

$$\inf\{\mathcal{T}_c^\lambda(G_M) : G_M \in \mathbb{G}_M\} \geq \inf\{\mathcal{J}_c^\lambda(G_M) : G_M \in \mathbb{G}_M\} \quad (16)$$

and

$$\inf\{\mathcal{T}_c^\lambda(G_M) : G_M \in \mathbb{G}_M\} \leq \inf\{\mathcal{J}_c^\lambda(G_M) : G_M \in \mathbb{G}_M\} \quad (17)$$

We first prove (16). Let $G^* = \arg \inf\{\mathcal{T}_c^\lambda(G_M) : G_M \in \mathbb{G}_M\}$. Denote the m th subpopulation and the corresponding mixing weight by Φ_m^* and w_m^* respectively. Let

$$\pi^* = \arg \inf \left\{ \sum_{n,m} \pi_{nm} c(\Phi_n, \Phi_m^*) - \lambda \mathcal{H}(\pi) : \pi \in \Pi(w, w^*) \right\}.$$

Then

$$\inf\{\mathcal{T}_c^\lambda(G_M) : G_M \in \mathbb{G}_M\} = \mathcal{T}_c^\lambda(G^*) = \sum_{n,m} \pi_{nm}^* c(\Phi_n, \Phi_m^*) - \lambda \mathcal{H}(\pi^*) \geq \mathcal{J}_c^\lambda(G^*) \geq \inf\{\mathcal{J}_c^\lambda(G_M) : G_M \in \mathbb{G}_M\}.$$

Next, we prove (17). Let $G^\dagger = \arg \inf\{\mathcal{J}_c^\lambda(G) : G \in \mathbb{G}_M\}$. Denote the m th subpopulation and the corresponding mixing weight by Φ_m^\dagger and w_m^\dagger respectively. Let

$$\pi^\dagger = \arg \inf \left\{ \sum_{n,m} \pi_{nm} c(\Phi_n, \Phi_m^\dagger) - \lambda \mathcal{H}(\pi) : \pi \in \Pi(w, \cdot) \right\}.$$

Then by definition, we have $w_m^\dagger = \sum_{n=1}^N \pi_{nm}^\dagger$. Clearly, $\pi^\dagger \in \Pi(w, w^\dagger)$, hence

$$\inf\{\mathcal{J}_c^\lambda(G_M) : G_M \in \mathbb{G}_M\} = \mathcal{J}_c^\lambda(G^\dagger) = \sum_{n,m} \pi_{nm}^\dagger c(\Phi_n, \Phi_m^\dagger) - \lambda \mathcal{H}(\pi^\dagger) \geq \mathcal{T}_c^\lambda(G^\dagger) \geq \inf\{\mathcal{T}_c^\lambda(G_M) : G_M \in \mathbb{G}_M\},$$

which completes the proof. \square

APPENDIX B
DETAILS RELATED TO MAJORIZATION-MINIMIZATION ALGORITHM

A. Optimal Transportation Plan with One Marginal Constraint

Let $\mathcal{H}(\pi) = -\sum_{n,m} \pi_{nm} (\log \pi_{nm} - 1)$ be the entropy of the transportation plan π and $\Pi(w, \cdot) = \{\pi = \{\pi_{nm}\} : \pi_{nm} \geq 0, \sum_{m=1}^M \pi_{nm} = w_n\}$. Denote

$$\pi^\lambda = \arg \inf \left\{ \sum_{n,m} \pi_{nm} C_{nm} - \lambda \mathcal{H}(\pi) : \pi \in \Pi(w, \cdot) \right\}.$$

for some $C_{nm} \geq 0$ that is known and does not depend on π . We show in this section that

$$\pi_{nm}^\lambda = \frac{w_n \exp(-C_{nm}/\lambda)}{\sum_{m'} \exp(-C_{nm'}/\lambda)}.$$

When $\lambda = 0$, $\pi_{nm}^0 = \lim_{\lambda \downarrow 0} \pi_{nm}^\lambda$.

Proof. Let

$$\ell_C(\pi) = \sum_{n,m} \pi_{nm} C_{nm} - \lambda \mathcal{H}(\pi). \quad (18)$$

We prove the results in the following two cases.

Case I ($\lambda > 0$) The Lagrangian associated with (18) is

$$\mathcal{L}(\pi, \xi_1, \dots, \xi_N) = \ell_C(\pi) - \sum_{n=1}^N \xi_n \left\{ \sum_{m=1}^M \pi_{nm} - w_n \right\}.$$

Then for $n = 1, 2, \dots, N$ and $m = 1, 2, \dots, M$, the first order conditions yield

$$\begin{cases} \frac{\partial \mathcal{L}}{\partial \pi_{nm}} = C_{nm} - \lambda \log \pi_{nm} - \xi_n = 0, \\ \frac{\partial \mathcal{L}}{\partial \xi_n} = \sum_{m=1}^M \pi_{nm} - w_n = 0. \end{cases}$$

The optimal transportation plan is the solution to the above equation:

$$\pi_{nm}^\lambda = \frac{w_n \exp(-C_{nm}/\lambda)}{\sum_{m'} \exp(-C_{nm'}/\lambda)}. \quad (19)$$

Case II ($\lambda = 0$) The objective function becomes

$$\ell_C(\pi) = \sum_{n,m} C_{nm} \pi_{nm}$$

which is linear in π under the constraints that $\sum_m \pi_{nm} = w_n$ for $n = 1, 2, \dots, N$. Suppose there are d_n elements in the set $I_n = \arg \min_{m'} C_{nm'}$. Therefore, by the linearity and the fact that $C_{nm} \geq 0$, it is clear that the objective function is smallest when

$$\pi_{nm} = \begin{cases} w_n/d_n & m = \arg \min_{m'} C_{nm'} \\ 0 & \text{otherwise} \end{cases}$$

We now show that when $\lambda \rightarrow 0$ and $\lim_{\lambda \downarrow 0} \pi_{nm}^\lambda = \pi_{nm}$. According to (19), we have

$$\lim_{\lambda \downarrow 0} \pi_{nm}^\lambda = \lim_{\lambda \downarrow 0} \frac{w_n \exp(-C_{nm}/\lambda)}{\sum_{m'} \exp(-C_{nm'}/\lambda)} = \lim_{\lambda \downarrow 0} \frac{w_n}{\sum_{m'} \exp\{-(C_{nm'} - C_{nm})/\lambda\}}$$

If $m \in I_n$ and $m^* \notin I_n$, then $\exp\{-(C_{nm^*} - C_{nm})/\lambda\} \rightarrow 0$ as $\lambda \downarrow 0$. If both $m, m^* \in I_n$, then $\exp\{-(C_{nm^*} - C_{nm})/\lambda\} = 1$. Therefore, the sum of the denominator equals d_n and $\lim_{\lambda \downarrow 0} \pi_{nm}^\lambda = w_n/d_n = \pi_{nm}$.

If $m \notin I_n$, there must exist an m^* such that $C_{nm^*} < C_{nm}$. Hence, $\exp\{-(C_{nm^*} - C_{nm})/\lambda\} \rightarrow \infty$ so the denominator goes to ∞ as $\lambda \downarrow 0$. Consequently, $\lim_{\lambda \downarrow 0} \pi_{nm}^\lambda \rightarrow 0 = \pi_{nm}$.

We have shown in both cases, the claim is true. This completes the proof. \square

B. Proof of Theorem 2

Proof. We first prove property 1). We have $\mathcal{K}_c^\lambda(G^\dagger | \tilde{G}^{(t)}) \geq \mathcal{J}_c^\lambda(G^\dagger)$ for all $G^\dagger \in \mathbb{G}_M$ with equality holds at $G^\dagger = \tilde{G}^{(t)}$. Hence,

$$\begin{aligned} \mathcal{J}_c^\lambda(\tilde{G}^{(t)}) &\geq \mathcal{J}_c^\lambda(\tilde{G}^{(t)}) - \{\mathcal{K}_c^\lambda(\tilde{G}^{(t+1)} | \tilde{G}^{(t)}) - \mathcal{J}_c^\lambda(\tilde{G}^{(t+1)})\} \\ &= \mathcal{J}_c^\lambda(\tilde{G}^{(t+1)}) - \{\mathcal{K}_c^\lambda(\tilde{G}^{(t+1)} | \tilde{G}^{(t)}) - \mathcal{J}_c^\lambda(\tilde{G}^{(t)})\} \\ &\geq \mathcal{J}_c^\lambda(\tilde{G}^{(t+1)}) - \{\mathcal{K}_c^\lambda(\tilde{G}^{(t)} | \tilde{G}^{(t)}) - \mathcal{J}_c^\lambda(\tilde{G}^{(t)})\} \\ &= \mathcal{J}_c^\lambda(\tilde{G}^{(t+1)}). \end{aligned}$$

This is the property that a majorization-minimization algorithm must have.

We now prove property 2). Suppose $\tilde{G}^{(t)}$ has a convergent subsequence leading to a limit \tilde{G}^* . Let this subsequence be $\tilde{G}^{(t_k)}$. By Helly's selection theorem [36], there is a subsequence s_k of t_k such that $\tilde{G}^{(s_k+1)}$ has a limit, say \tilde{G}^{**} . These limits, however, could be subprobability distributions. That is, we cannot rule out the possibility that the total probability in the limit is below 1 by Helly's theorem.

This is not the case under the theorem conditions. Let $\Delta > 0$ be large enough such that

$$A_1 = \{\Phi : c(\Phi_n, \Phi) \leq \Delta, \text{ for all subpopulations } \Phi_n \text{ of } G\}$$

is not empty. With this Δ , we define

$$A_2 = \{\Phi : c(\Phi_n, \Phi) > \Delta, \text{ for all subpopulations } \Phi_n \text{ of } G\}.$$

Suppose G^\dagger has a subpopulation Φ^\dagger such that $c(\Phi_n, \Phi^\dagger) > \Delta$ for all n . Replacing this subpopulation in G^\dagger by any $\Phi^{\dagger\dagger} \in A_1$ to form $G^{\dagger\dagger}$, we can see that for any t ,

$$\mathcal{K}_c^\lambda(G^\dagger | \tilde{G}^{(t-1)}) > \mathcal{K}_c^\lambda(G^{\dagger\dagger} | \tilde{G}^{(t-1)}).$$

This result shows that none of the subpopulations of $G^{(t)}$ are members of A_2 . Otherwise, $\tilde{G}^{(t)}$ does not minimize $\mathcal{K}_c(\tilde{G} | \tilde{G}^{(t-1)})$ at the t th iteration.

Note that the complement of A_2 is compact by condition

$$\{\Phi : c(\Phi^*, \Phi) \leq \Delta\}.$$

Consequently, the subpopulations of $\tilde{G}^{(t)}$ are confined to a compact subset. Hence, all limit points of $\tilde{G}^{(t)}$, including both \tilde{G}^* and \tilde{G}^{**} , are proper distributions. By the monotonicity of the iteration:

$$\mathcal{J}_c^\lambda(\tilde{G}^{(s_{k+1})}) \leq \mathcal{J}_c^\lambda(\tilde{G}^{(s_k+1)}) \leq \mathcal{J}_c^\lambda(\tilde{G}^{(s_k)}).$$

Let $k \rightarrow \infty$, we get

$$\mathcal{J}_c^\lambda(\tilde{G}^{**}) = \mathcal{J}_c^\lambda(\tilde{G}^*). \quad (20)$$

By the definition of the majorization-minimization iteration, we have

$$\mathcal{K}_c^\lambda(\tilde{G}^{(s_{k+1})} | \tilde{G}^{(s_k)}) \leq \mathcal{K}_c^\lambda(\tilde{G} | \tilde{G}^{(s_k)}).$$

Let $k \rightarrow \infty$ and by the continuity of $\mathcal{K}_c^\lambda(\cdot | \cdot)$, we get

$$\mathcal{K}_c(\tilde{G}^{**} | \tilde{G}^*) \leq \mathcal{K}_c(\tilde{G} | \tilde{G}^*).$$

Hence, \tilde{G}^{**} is a solution to $\min \mathcal{K}_c^\lambda(\tilde{G} | \tilde{G}^{(t)})$ when $\tilde{G}^{(t)} = \tilde{G}^*$. Namely, we have $\mathcal{K}_c^\lambda(\tilde{G}^{**} | \tilde{G}^*) = \mathcal{K}_c^\lambda(\tilde{G}^{(t+1)} | \tilde{G}^*)$. With the help of (20), it further implies

$$\mathcal{J}_c^\lambda(\tilde{G}^{**}) = \mathcal{J}_c^\lambda(\tilde{G}^{(t+1)}) = \mathcal{J}_c^\lambda(\tilde{G}^*)$$

when $\tilde{G}^{(t)} = \tilde{G}^*$. This shows that iteration from $\tilde{G}^{(t)} = \tilde{G}^*$ does not make $\mathcal{J}_c^\lambda(\tilde{G}^{(t+1)})$ smaller than $\mathcal{J}_c^\lambda(\tilde{G}^{(t)})$. Hence, \tilde{G}^* is a stationary point of the majorization-minimization iteration. This is the conclusion (ii) and we have completed the proof.

Finally, when $\lambda = 0$, the proposed algorithm is a member of hard clustering-based. The eventual solution is to divide the N subpopulations of the original mixture into M clusters, followed by finding the total weight of each cluster and its barycenter. Since there are M^N possible different clustering outcomes, we have at most M^N different $\mathcal{J}_c^0(\tilde{G}^{(t+1)})$ values. By the monotonicity of $\mathcal{J}_c^0(\tilde{G}^{(t+1)})$, the MM-algorithm must stall after a finite number of iterations. In other words, it converges after at most M^N iterations. \square

When M^N is not large, one may compute all possible $\mathcal{J}_c^0(G)$ values to locate the global optimal solution. This is infeasible in all examples in our experiment section. We do not know if the MM algorithm has a similar property when $\lambda > 0$.

APPENDIX C

GAUSSIAN BARYCENTER UNDER DIFFERENT DIVERGENCES

The key to the update step of our composite transportation divergence based approach for Gaussian mixture reduction is to find out the barycenter of Gaussian distributions under various divergences. The barycenter of the Gaussian distributions with respect to some divergence has either an explicit solution or permits simple numerical solution. We give an overview of the Gaussian barycenter under squared Wasserstein distance and KL divergence.

Let $\Phi_n(x) = \Phi(x; \mu_n, \Sigma_n)$ and $(\lambda_1, \lambda_2, \dots, \lambda_N)$ be a vector of positive values of length N . The (weighted) barycenter of Gaussian distributions $\Phi_1, \Phi_2, \dots, \Phi_N$ is defined to be

$$\bar{\Phi} = \arg \min_{\Phi \in \mathcal{F}} \sum_{n=1}^N \lambda_n \rho(\Phi_n, \Phi) \quad (21)$$

where \mathcal{F} is the space of all Gaussian distributions.

The barycenter depends on the divergence ρ and the weights. For simplicity, we will omit the information on the weights in the name but specify the divergence.

Wasserstein barycenter of Gaussians

When the divergence $\rho(\Phi_n, \Phi) = W_2^2(\Phi(\cdot; \theta_n), \Phi(\cdot; \theta))$, it is shown in [31] that the Wasserstein barycenter $\bar{\Phi}$ in (21) has mean $\bar{\mu} = \sum_{n=1}^N \lambda_n \mu_n$ and covariance $\bar{\Sigma}$ is the unique positive definite matrix root of the following equation

$$\sum_{n=1}^N \lambda_n \left(\Sigma^{1/2} \Sigma_n \Sigma^{1/2} \right)^{1/2} = \Sigma. \quad (22)$$

In our update step of the algorithm, we use the fixed point iteration

$$\Sigma_{(t+1)} = \sum_{n=1}^N \lambda_n \left(\Sigma_{(t)} \Sigma_n \Sigma_{(t)} \right)^{1/2},$$

where $\Sigma_{(t)}$ is the covariance matrix at t th step, to find the solution to (22).

Kullback-Leibler barycenter of Gaussians

When the divergence $\rho(\Phi_n, \Phi) = D_{\text{KL}}(\Phi(\cdot; \theta_n) \| \Phi(\cdot; \theta))$, then the KL barycenter $\bar{\Phi}$ has mean $\bar{\mu} = \sum_{n=1}^N \lambda_n \mu_n$ and covariance matrix

$$\bar{\Sigma} = \sum_{n=1}^N \lambda_n (\Sigma_n + (\mu_n - \bar{\mu})(\mu_n - \bar{\mu})^\top).$$

We prove the conclusion below.

Proof. With KL divergence, the barycenter in the space of Gaussians is a Gaussian with its mean and covariance minimizing the function

$$L(\mu, \Sigma) = \sum_{n=1}^N \lambda_n D_{\text{KL}}(\Phi_n \| \Phi) = \frac{1}{2} \sum_n \lambda_n \{ \log \det(\Sigma) + \text{tr}(\Sigma^{-1} \Sigma_n) \} + \frac{1}{2} \sum_n \lambda_n (\mu - \mu_n)^\top \Sigma^{-1} (\mu - \mu_n) + \text{const.}$$

We now use the following linear algebra formulas

$$\begin{aligned} \frac{\partial \log \det(\Sigma)}{\partial \Sigma} &= (\Sigma^{-1})^\top = (\Sigma^\top)^{-1}, \\ \frac{\partial \text{tr}(A \Sigma^{-1} B)}{\partial \Sigma} &= -(\Sigma^{-1} B A \Sigma^{-1})^\top, \end{aligned}$$

and

$$\frac{\partial}{\partial x} (x - \mu)^\top \Sigma^{-1} (x - \mu) = 2 \Sigma^{-1} (x - \mu)$$

to work out partial derivatives of L with respect to μ and Σ . They are given by

$$\begin{aligned} \frac{\partial L}{\partial \mu} &= 2 \sum_n \lambda_n \Sigma^{-1} (\mu - \mu_n), \\ \frac{\partial L}{\partial \Sigma} &= \Sigma^{-1} - \Sigma^{-1} \sum_n \lambda_n \{ \Sigma_n + (\mu - \mu_n)(\mu - \mu_n)^\top \} \Sigma^{-1}. \end{aligned}$$

Setting both partial derivatives to 0, we obtain

$$\bar{\mu} = \left\{ \sum_n \lambda_n \right\}^{-1} \sum_{n=1}^N \lambda_n \mu_n$$

and the covariance

$$\bar{\Sigma} = \left\{ \sum_n \lambda_n \right\}^{-1} \sum_{n=1}^N \lambda_n \{ \Sigma_n + (\mu_n - \bar{\mu})(\mu_n - \bar{\mu})^\top \}.$$

This completes the proof. □

REFERENCES

- [1] C. Fraley and A. E. Raftery, "Model-based clustering, discriminant analysis, and density estimation," *Journal of the American Statistical Association*, vol. 97, no. 458, pp. 611–631, 2002.
- [2] V. Melnykov and R. Maitra, "Finite mixture models and model-based clustering," *Statistics Surveys*, vol. 4, pp. 80–116, 2010.
- [3] C. Bouveyron and C. Brunet-Saumard, "Model-based clustering of high-dimensional data: A review," *Computational Statistics & Data Analysis*, vol. 71, pp. 52–78, 2014.
- [4] K. Moshksar and A. K. Khandani, "Arbitrarily tight bounds on differential entropy of gaussian mixtures," *IEEE Transactions on Information Theory*, vol. 62, no. 6, pp. 3340–3354, 2016.
- [5] G. McLachlan and D. Peel, *Finite Mixture Models*. John Wiley & Sons, 2004.
- [6] T. T. Nguyen, H. D. Nguyen, F. Chamroukhi, and G. J. McLachlan, "Approximation by finite mixtures of continuous density functions that vanish at infinity," *Cogent Mathematics & Statistics*, vol. 7, no. 1, p. 1750861, 2020.
- [7] D. M. Titterton, S. Afm, A. F. Smith, and U. Makov, *Statistical Analysis of Finite Mixture distributions*. John Wiley & Sons Incorporated, 1985, vol. 198.
- [8] E. B. Sudderth, A. T. Ihler, M. Isard, W. T. Freeman, and A. S. Willsky, "Nonparametric belief propagation," *Communications of the ACM*, vol. 53, no. 10, pp. 95–103, 2010.
- [9] M. A. Brubaker, A. Geiger, and R. Urtasun, "Map-based probabilistic visual self-localization," *IEEE Transactions on Pattern Analysis and Machine Intelligence*, vol. 38, no. 4, pp. 652–665, 2015.
- [10] L. Yu, T. Yang, and A. B. Chan, "Density-preserving hierarchical EM algorithm: simplifying Gaussian mixture models for approximate inference," *IEEE Transactions on Pattern Analysis and Machine Intelligence*, vol. 41, no. 6, pp. 1323–1337, 2018.
- [11] D. J. Salmond, "Mixture reduction algorithms for target tracking in clutter," in *Signal and Data Processing of Small Targets 1990*, vol. 1305. International Society for Optics and Photonics, 1990, p. 434.
- [12] A. R. Runnalls, "Kullback-Leibler approach to Gaussian mixture reduction," *IEEE Transactions on Aerospace and Electronic Systems*, vol. 43, no. 3, pp. 989–999, 2007.
- [13] J. L. Williams and P. S. Maybeck, "Cost-function-based hypothesis control techniques for multiple hypothesis tracking," *Mathematical and Computer Modelling*, vol. 43, no. 9–10, pp. 976–989, 2006.
- [14] M. F. Huber and U. D. Hanebeck, "Progressive Gaussian mixture reduction," in *2008 11th International Conference on Information Fusion*. IEEE, 2008, pp. 1–8.
- [15] N. Vasconcelos and A. Lippman, "Learning mixture hierarchies," in *Advances in Neural Information Processing Systems 11*, 1999, pp. 606–612.
- [16] J. Goldberger and S. T. Roweis, "Hierarchical clustering of a mixture model," in *Advances in Neural Information Processing Systems 17*, 2005, pp. 505–512.
- [17] J. V. Davis and I. S. Dhillon, "Differential entropic clustering of multivariate Gaussians," in *Advances in Neural Information Processing Systems 19*, 2007, pp. 337–344.
- [18] A. Assa and K. N. Plataniotis, "Wasserstein-distance-based Gaussian mixture reduction," *IEEE Signal Processing Letters*, vol. 25, no. 10, pp. 1465–1469, 2018.
- [19] D. Schieferdecker and M. F. Huber, "Gaussian mixture reduction via clustering," in *2009 12th International Conference on Information Fusion*. IEEE, 2009, pp. 1536–1543.
- [20] K. Zhang and J. T. Kwok, "Simplifying mixture models through function approximation," *IEEE Transactions on Neural Networks*, vol. 21, no. 4, pp. 644–658, 2010.
- [21] D. F. Crouse, P. Willett, K. Pattipati, and L. Svensson, "A look at Gaussian mixture reduction algorithms," in *14th International Conference on Information Fusion*. IEEE, 2011, pp. 1–8.
- [22] S. Lloyd, "Least squares quantization in pcm," *IEEE transactions on information theory*, vol. 28, no. 2, pp. 129–137, 1982.
- [23] X. Nguyen, "Convergence of latent mixing measures in finite and infinite mixture models," *The Annals of Statistics*, vol. 41, no. 1, pp. 370–400, 2013.
- [24] Y. Chen, T. T. Georgiou, and A. Tannenbaum, "Optimal transport for Gaussian mixture models," *IEEE Access*, vol. 7, pp. 6269–6278, 2018.
- [25] M. West, "Approximating posterior distributions by mixtures," *Journal of the Royal Statistical Society: Series B (Methodological)*, vol. 55, no. 2, pp. 409–422, 1993.
- [26] J. L. Williams, "Gaussian mixture reduction of tracking multiple maneuvering targets in clutter," Master's thesis, Air Force Institute of Technology, 2003.
- [27] C. Villani, *Topics in Optimal Transportation*. American Mathematical Society, 2003, vol. 58.
- [28] J. Delon and A. Desolneux, "A Wasserstein-type distance in the space of Gaussian mixture models," *SIAM Journal on Imaging Sciences*, vol. 13, no. 2, pp. 936–970, 2020.
- [29] G. Peyré and M. Cuturi, "Computational optimal transport: with applications to data science," *Foundations and Trends®*

- in *Machine Learning*, vol. 11, no. 5–6, pp. 355–607, 2019.
- [30] D. R. Hunter and K. Lange, “A tutorial on MM algorithms,” *The American Statistician*, vol. 58, no. 1, pp. 30–37, 2004.
 - [31] M. Agueh and G. Carlier, “Barycenters in the Wasserstein space,” *SIAM Journal on Mathematical Analysis*, vol. 43, no. 2, pp. 904–924, 2011.
 - [32] D. M. Blei, A. Kucukelbir, and J. D. McAuliffe, “Variational inference: A review for statisticians,” *Journal of the American statistical Association*, vol. 112, no. 518, pp. 859–877, 2017.
 - [33] J. Triesch and C. Von Der Malsburg, “Robust classification of hand postures against complex backgrounds,” in *Proceedings of the Second International Conference on Automatic Face and Gesture Recognition*. IEEE, 1996, pp. 170–175.
 - [34] K. Kampa, E. Hasanbelliu, and J. C. Principe, “Closed-form Cauchy-Schwarz pdf divergence for mixture of Gaussians,” in *The 2011 International Joint Conference on Neural Networks*. IEEE, 2011, pp. 2578–2585.
 - [35] R. Jenssen, J. C. Principe, D. Erdogmus, and T. Eltoft, “The Cauchy–Schwarz divergence and Parzen windowing: connections to graph theory and Mercer kernels,” *Journal of the Franklin Institute*, vol. 343, no. 6, pp. 614–629, 2006.
 - [36] A. W. Van der Vaart, *Asymptotic Statistics*. Cambridge University Press, 2000, vol. 3.